DYNAMIC PROPERTIES OF TIRE-DERIVED AGGREGATES

Ahmed Moussa & Hany El Naggar.
Department of Civil & Resource Engineering, Dalhousie University, Halifax, Nova Scotia, Canada

ABSTRACT
There are approximately 35 million scrap tires generated per year in Canada. Around 30% of which, end up in stockpiles that occupy large landfill space causing several environmental and public health problems. Therefore, utilizing these waste materials is vital for environmental, health and economical improvements. Consequently, in the recent past, there has been an increasing need to study and investigate the behaviour of Tire Derived Aggregate (TDA) and its usage in various civil engineering applications. Several experimental studies were carried out to investigate the behaviour of TDA under monotonic loading and cyclic loading. However, the experimental work regarding the dynamic behaviour of Type A TDA is not yet addressed. Therefore, the scope of this study is to investigate the dynamic behaviour of TDA under cyclic loading. A strain controlled consolidated undrained large-scale cyclic triaxial test is carried out to obtain the dynamic properties of TDA under confinement pressures of 100 and 200 KPa. A staged loading was applied to all specimens for 0.5%, 1%, 2%, 5%, 7.5% and 10% shear strain amplitudes. This paper presents the experimental work results, including the shear modulus and dampening ratio variations with shear strain for Type A TDA. This is a research in progress, and more results on different confining pressures will be provided later.

ABSTRAITE
Il y a environ 35 millions de pneus usagés produits chaque année au Canada. Parmi eux, 30% se retrouvent dans des déchèteries qui occupent de vastes terrains, ce qui pose une multitude de problèmes environnementaux et de santé publique. Par conséquent, trouver une utilisation alternative de ces déchets est essentielle pour l'amélioration de l'environnement, de la santé et de l'économie. En conséquence, il y a eu récemment un besoin croissant d'étudier et d'analyser le comportement des agrégat dérivés de pneus (abrégé TDA de l'anglais Tyre Derived Aggregate) et son utilisation dans diverses applications du génie civil. Plusieurs études expérimentales ont été menées pour étudier le comportement du TDA sous chargement monotone et chargement cyclique. Cependant, les travaux expérimentaux sur le comportement dynamique de la TDA de type A n'ont pas encore été abordés. Par conséquent, l'objectif de cette étude est d'étudier le comportement dynamique du TDA soumis à une charge cyclique. Plus précisément, un essai triaxial cyclique à grande échelle, non drainé, consolidé et sous déformations contrôlées est réalisé pour obtenir les propriétés dynamiques du TDA sous des pressions de confinement de 100 et 200 KPa. Un chargement a été appliqué à tous les échantillons, par échelons, afin d'obtenir des amplitudes de déformation de cisaillement de 0,5%, 1%, 2%, 5%, 7,5% et 10%. Cet article présente les résultats des travaux expérimentaux, y compris les variations du module de cisaillement et du coefficient d'amortissement en fonction de la déformation au cisaillement, pour le TDA de type A. Cette recherche est en cours, et plus de résultats sur l'effet de différentes pressions de confinement seront fournis ultérieurement.

1 INTRODUCTION

Every year, the number of tires disposed of in Nova Scotia equals the number of residents within the province. Meanwhile, in Alberta, around five million tires are disposed of annually. With the increase in the Canadian population, the number of disposed of tires will rise proportionately (Meles et al. 2015). Landfilling scrap tires is no longer allowed in Nova Scotia due to its environmental and health hazards (Edinçliler et al., 2010).

Stockpiling tires takes up massive landfill space, and as land is becoming increasingly scarce, it may cause illegal dumping. Tires have great potential for tire fires that are inextinguishable and, in some instances, they can burn for several weeks. Tires pose a health hazard, as they serve as a breeding ground for mosquitoes.

Fortunately, there are several methods available for reusing scrap tires. The main method for reusing scrap tires in civil engineering applications is to shred tires into small pieces referred to as tire derived aggregates (TDA). For example, it is used as a light backfill for embankments, retaining walls and around buried pipes and culverts. The two types of TDA are Type A (maximum aggregate size is less than or equal to 200 mm) and Type B (maximum aggregate size is less than or equal to 400 mm). Scrap tires are also used as Tire-Derived Fuel (TDF) because of their high heat value, which is higher than coal. Last but not least, they are utilized in ground rubber application like in children playgrounds. The properties of TDA must be identified in order for this product to be utilized in civil engineering projects with confidence. With the use of TDA on the rise, research has had difficulty keeping up with the demand (Ashari, 2018).

Several studies have discussed in detail, the static and cyclic behavior of small TDA particles (less than 2 mm) mixed with natural soils (Masad et al. 1996; Wu et al. 1997; Zornberg et al. 2004; Feng and Sutter 2000; Kaneko et al. 2013; Mashiri et al. 2016; Madhusudhan et al. 2017). However, the dynamic properties of Type A TDA under cyclic loading have not yet been addressed. ASTM D6270 recommended the use of Type A for drainage, vibration dampening and insulation for civil engineering applications. Some of these applications are seismic isolation for building foundations, mitigation of liquefaction at coastal

areas and vibration dampening from compaction (McCartney et al. 2017). Therefore, the present paper represents the results of large scale cyclic triaxial tests for Type A TDA. The results include shear modulus and dampening ratio variation with shear strain.

2 BACKGROUND

2.1 Previous laboratory studies on the dynamic behaviour of TDA

One of the earliest investigations regarding the dynamic behaviour of TDA was done by Feng and Sutter, (2000). The authors investigated the shear modulus degradation and damping ratios for various rubber/soil mixtures and rubber only, using a torsional resonant column that could accommodate a specimen size that is 7 cm in diameter and 15 cm in height. The used granulated rubber had a specific gravity of 1.11 and a void ratio of 0.35 at 69 KPa. The particle sizes of the granulated rubber were between 2 mm and 4.76 mm. Four different confining pressures were used, i.e. 69, 207, 345 and 483 KPa. It was concluded that as the percentage of rubber increased in the rubber-sand mixture, the shear modulus degradation becomes insignificant. Furthermore, for 100% of rubber sample, the shear modulus degradation is almost linear. Also, as the confining pressure increases for the 100% rubber sample, the damping ratio tends to increase slightly due to the ability of the rubber particles to consume energy through its deformation. This behaviour differentiates the damping capability of rubber particles because it contradicts the response of the conventional soil.

Hazarika et al. (2010) studied the performance of tire chips and sand-tire chips mixtures under cyclic loading using undrained triaxial cyclic test. The maximum particle size of the tire chips was 1 mm. It was found that the behaviour of pure tire chips under cyclic loading is viscoelastic. Furthermore, the axial strain for the first cycle was much greater than the axial strain for the subsequent cycles. Also, there was almost no excess pore water pressure generated, which indicates the advantage of tire chips to control/prevent liquefaction. However, it was noted that due to the low stiffness of the tire chips, excessive deformations were observed under the prescribed loading. Finally, the authors performed a shaking table test to demonstrate the effect of using sand-tire chips mixtures as a backfill material for retaining walls to control liquefaction. The test revealed that when a mixture of 50% tire chips and 50% sand by volume was used as backfill, the tire chips significantly reduced the excess pore water pressure build up and prevented any damages associated with liquefaction.

It is shown from the aforementioned studies that the dynamic properties of TDA were found for aggregate sizes ranging from 1 mm to 4.76 mm, which are not the typical aggregate sizes that are used in civil construction. Therefore, McCartney et al. (2017) addressed this issue by conducting a large scale cyclic simple shear test on type B TDA, which had a maximum aggregate size of 320 mm. The shear modulus degradation and the dampening characteristics of Type B TDA were found for shear strain levels ranging from 0.1% to 10% and vertical stress ranging from 19.3 to 76.6 KPa. The reported range of shear modulus was 155 to 2,386 kPa, which is within the reported shear modulus values by Feng and Sutter, (2000), and Hazarika et al. (2010). Furthermore, the damping ratio range at 0.1% shear strain was found to be in the range of 21 to 26.8%, which indicates the significant damping capacity of TDA in comparison to granular soils. In addition, Madhusudhan et al. (2019) performed a series of strain-controlled undrained cyclic triaxial tests for tire shred of a maximum size of 2 mm. The shear modulus values, i.e. from 1 MPa to 2.25 MPa, were in a good agreement with what McCartney et al. (2017) presented. However, regarding the damping ratios, pure tire shreds had the lowest damping ratio of around 10%, which was lower than the damping ratio of pure sand, i.e. around 16.25% to 23.75%.

2.2 Previous studies on numerical modelling of TDA

Due to the increase of the computational power of computers and the development of advanced finite element (FE) and discrete element (DE) software, numerous researchers are investigating at the micro and macro levels the dynamic and static properties of pure tire and sand-tire mixtures. DE method was mainly used by researchers to gain deeper insights regarding the microscale behaviour and the internal mechanism of rubber-rubber particles and rubber-sand particles.

For instance, Lee et al. (2014) used the DE method to simulate the behaviour of pure rubber and rubber-sand mixtures. A series of dynamic resonant column tests and direct shear tests were used to calibrate the numerical model. The simulations revealed important aspects regarding the effect of adding rubber particles into the sand. First, at low shear strain levels, the rubber particles significantly increased the sand particles coordination (i.e., the particles orientation were uniform and provided a well compacted sample) and controlled the behaviour of the whole mixture. Second, at medium shear strain levels, the rubber particles effectively prevented the buckling failure of the mixture during testing. Third, at high shear strain levels, with increasing the rubber particles percentage in the mixture, the mixture showed a contractive behaviour.

Similarly, Takano et al. (2015) conducted a series of direct shear tests on tire-chips and mixtures of tire-chips and silica-sand to obtain the shear parameters. Then, a 3D DE model was created to simulate the laboratory results. For the case of pure tire-chips, the DE model and laboratory tests showed almost linear behaviour. However, Ashari (2018) showed that the behaviour of tires is nonlinear based on an extensive study using large-scale triaxial tests. Moreover, the reason for the monotonic increase of the stress-strain could be due to the size of tire-crumbs (2 mm) and the absence of steel wires. The DE models of Takano et al. (2015) showed that the tire-chips had a contractive behaviour which agrees with the findings of Lee et al. (2014). Finally, there was a gap between the simulated behaviour of pure sand and the lab results which implies the inability of the DE model to simulate the shear behaviour of sand. However, there was a good agreement

between the DE model and the lab results for the pure tire-chips case.

Asadi et al. (2018) successfully developed a new technique to accurately model the behaviour of pure tire-crumbs and sand-crumb mixtures by using the DE model. Unlike the previous studies, Asadi et al. (2018) models had the best agreement between the results of the simulation models and the laboratory results. The key feature for the author's model is the consideration of both shape and deformability of tire-crumbs and sand grains. Tire-crumbs were modelled as deformable agglomerate, whereas, the sand grains were modelled as a rigid agglomerate. The reason behind selecting the previously mentioned approaches for modelling the tire-crumbs and sand grains is to create a contact area between the two grains, which have a high difference in stiffness, rather than a single contact point. In return, this approach significantly affected the overall behaviour of the whole model, which yielded results that are in close agreement with the conducted compression triaxial test results. In addition, the simulations showed that by adding tire-crumbs to the sand, the stiffness and the dilative behaviour of the samples decreased significantly.

On the other hand, the FE method was used by many types of research to study the possibility of using rubber and rubber-sand mixtures as a lightweight backfill for retaining structures or embankments. The authors (Lee et al. 1991) compare the strength and the stress-strain relationship of tire chips and a combination of sand and tire chips, through a triaxial testing program. Isotropic compression tests on tire-chip triaxial samples and the volumetric and stress-strain behaviour under triaxial loading have shown that escalating confining pressure results in significant volume reduction and unit weight change in the sample. In order to ensure reliability, these effects must be taken into account when designing a tire-shred numerical model. The authors used ABAQUS to conduct the finite-element analysis of the tire-shred fill. However, it has been observed that finite-element strategies overestimate the lateral pressure on the wall with a tire-shred backfill. This can be caused by the limited ability of the hyperbolic model to imitate the tight coupling of tire-shreds. Overall, the finite-element analysis estimations of deformations and stresses for a tire-shred backfill under at-rest condition are more realistic than the estimate of the active condition which was overvalued.

Meles et al. (2015) on the other hand, consider nonlinear elastic material models which are designed for TDA from passenger and light truck tire (PLTT) and off-the-road (OTR) vehicle tires based on prior large-scale, one-dimensional compression tests for TDA of sizes up to 300 mm. The PLTT and OTR are type B TDA. However, PLTT was used as Type A TDA for insulation. Finite-element analysis has been used to validate the material models. While the results show good agreement between finite-element and field measurements, an underestimation of up to 10% in the predictions of settlements in the PLTT sections is observed when compared with field measurements. This discrepancy is a result of developing the material model from large-scale compression tests which may differ from field compaction. Furthermore, OTR comprises bulky pieces as it is produced from tires of bigger sizes, which renders field compression more efficient than laboratory apparatus. This can be the cause of the overestimation of 7% observed in the OTR section.

3 TEST EQUIPMENT AND MATERIAL

3.1 Triaxial Test Equipment

Figure 1 shows the large scale cyclic triaxial test apparatus and the two volume-pressure controllers which were used to conduct the experimental work. The triaxial cell is capable of accommodating a sample which has a diameter of 152.4 mm and a height of 310 mm. Thus, the height to diameter ratio was 2, which satisfies the requirements of ASTM D3999/D3999M-11. The specimen top platen was fixed with the load shaft using a hard lock system, i.e. by using straight threads. The two advanced GDS pressure-volume controllers were calibrated and kept at the same level to obtain an accurate measurement for the cell and pore water pressures.

3.2 Material

The TDA used herein were manufactured by Halifax C&D ltd. Any protruding steel was completely removed in order to prevent membrane puncture. In addition, The TDA was sieved according to ASTM C136/C136M - 14. The sample had a TDA particle sizes ranges from 9.53 mm to 38.1 mm, as shown in Figure 2. It was found that the TDA falls under the Type A TDA category. Furthermore, the Coefficients of Uniformity (Cu) and Curvature (Cc) was found to be 2.32 and 0.76, respectively.

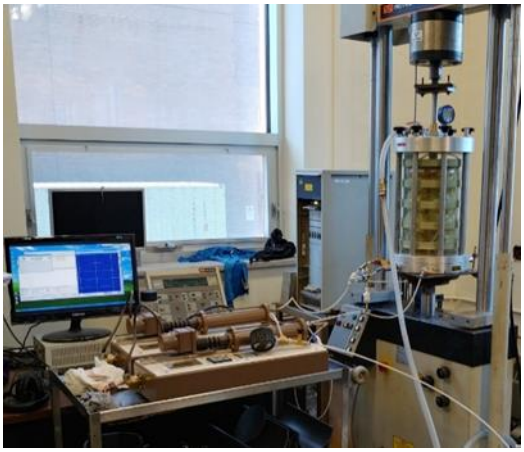

Figure 1. Cyclic triaxial test apparatus, load frame and volume-pressure controllers

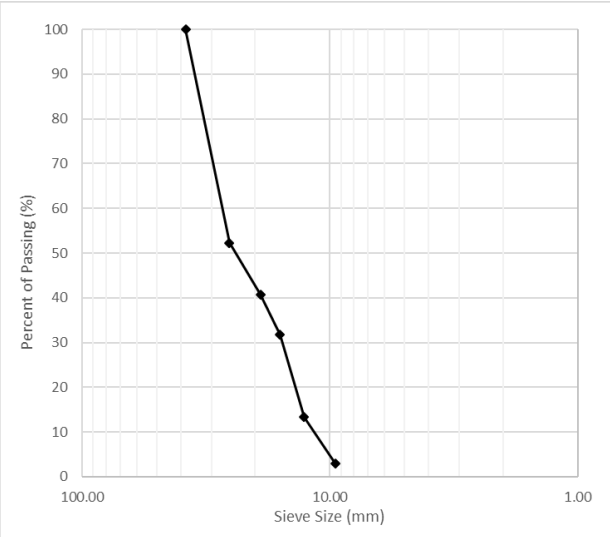

Figure 2. Sieve analysis for 38.1 mm Sample

3.3 Testing Scheme and Sample Preparation

3.3.1 Testing Scheme

Undrained confined large-scale cyclic triaxial tests were conducted in this study under strain-controlled conditions. A staged deformation loading was applied at different confining pressures, i.e. 100 KPa and 200 KPa. The selected strain levels were 0.5%, 1%, 2%, 5%, 7.5% and 10%. The testing scheme is summarized in Table 1 and consisted of four stages; each stage represents a certain shear strain level. The number of cycles for each stage was determined based on the number of cycles that will result in an almost constant shear modulus value. It is recommended by ASTM D3999/D3999M-11 to ensure that there is no excess of pore water pressure generated after each stage. Therefore, after each stage, 20 cycles with a very small axial deformation were applied to control the excess pore water pressure build up. However, it was found that there is no any excess pore water pressure generation between the first three stages because of the small magnitude of the axial deformation applied. Thus, the 20 cycles were not applied. All the tests were performed under a loading frequency of 0.5 Hz.

3.3.2 Sample Preparation

All the specimens had a height of 310 mm and a diameter of 152.4 mm. Special attention in protecting the membranes from puncturing was given by removing all the protruding steel wires. This practice eventually protected the membrane during the compaction of specimens, consolidation and shear testing phases. Furthermore, it will yield more conservative results because of the absence of the extra cohesion from the interlocking of the steel wires (Asharei, 2018). The TDA specimens were compacted to a total energy of 60% of standard Proctor energy. According to ASTM D6270-17, the range of the compaction energy for TDA is from 60% of standard proctor energy to 100% of modified proctor energy. However, 60% of standard Proctor energy is permissible to be used for most of the applications. To achieve the required compaction energy, the TDA were placed in five layers inside a split mould. Each layer was compacted by the modified proctor hammer and was given 20 blows. All specimens were prepared in dry conditions since the dry density of the TDA is not significantly influenced by introducing water, (Kowalska, 2016). A 0.635 mm thick latex membrane was used. This membrane is considered as a thick membrane, since a thinner membrane will not hold the high confining pressures and the relatively high number of cycles during the test. Figure 3 shows a prepared specimen before conducting the test.

Table 1. Summary of the cyclic triaxial test program

Test	Shear Strain Levels (%)	Confining Pressure (KPa)	Total Number of Cycles
CT1	0.5, 1, 2, 5, 7.5, 10	100	1700
CT2	0.5, 1, 2, 5, 7.5, 10	200	1700

4 EXPERIMENTAL RESULTS AND DISCUSSION

The output of the cyclic triaxial test is a series of hysteresis load-deformation loops as shown in Figure 4. It can be shown that as the deformation increases, the recorded axial load also increases. The next step is to convert the axial load-axial deformation hysteresis loops to deviatoric stress versus axial strain hysteresis curves. This can be done by using Eq.1, Eq.2, Eq. and Eq.4.

$$A_c = (V_o - \Delta V_s - \Delta V_c)/H_c \quad [1]$$

$$\Delta V_s = (3V_o\, \Delta H_s)/H_o \quad [2]$$

$$\sigma_d = F/A_c \quad [3]$$

$$\varepsilon_a = S/H_c \quad [4]$$

where A_c = Area of specimen after consolidation, V_o = initial volume of specimen, ΔV_s = change in volume of specimen during saturation, ΔH_s = change of specimen height during saturation, ΔV_c = change in specimen volume during consolidation, H_c = specimen height after consolidation, σ_d = deviatoric stress, F = recorded axial load, S = recorded axial deformation, ε_a = axial strain.

Then, the slope of the deviatoric stress versus axial strain was used to calculate the secant modulus (E_{sec}) as follows:

$$E_{sec} = \frac{\sigma_d^{max} - \sigma_d^{min}}{\varepsilon_a^{max} - \varepsilon_a^{min}} \quad [5]$$

Furthermore, the obtained E_{sec} then used to calculate the secant shear modulus (G_{sec}) using Eq.6. Also, the shear strain (γ) is obtained from axial strain as given by Eq.7. Finally, the damping ratio ($D(\%)$) for each hysteretic loop may be obtained by applying Eq.8.

$$G_{sec} = \frac{E_{sec}}{2(1+\mu)} \quad [6]$$

$$\gamma = \varepsilon_a(1+\mu) = \frac{3}{2}\varepsilon_a \quad [7]$$

$$D\ (\%) = \frac{1}{4\pi}\frac{A_{loop}}{A_{triangle}} \quad [8]$$

where A_{loop} = area of the hysteretic loop which represents the amount of energy dissipation of one loading cycle, $A_{triangle}$ = the stored elastic energy which is area of the shaded triangle in Figure 5.

A MATLAB (R2018b) code was developed to perform the calculations of E_{sec}, G_{sec} and $D\ (\%)$ for each test using the previously mentioned equations due to the enormous amount of data for each test.

Figure 3. A prepared TDA specimen

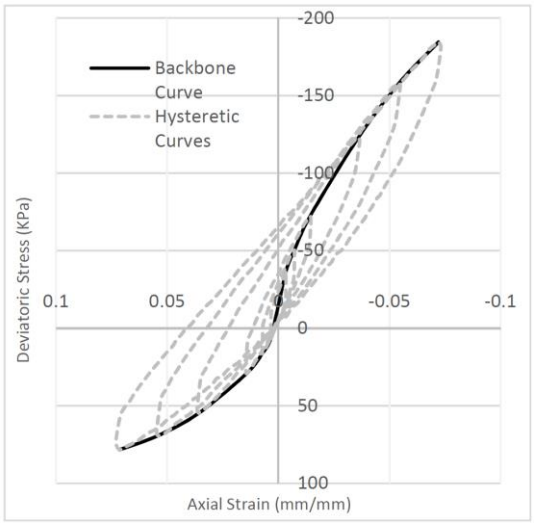

Figure 4. Backbone curve and its corresponding hysteretic loops for CT1 test

4.1 Backbone Curves

The backbone curves were obtained for the four tests by plotting the maximum deviatoric stresses versus the corresponding axial strains. Figure 4 shows the obtained backbone curve for CT1 test and its corresponding deviatoric stress versus axial strain hysteretic loop. The comparison of the backbone curves for both tests are shown in Figure 6. The work of Youwai and Bergado (2003), Masad et al. (1996), Lee et al. (1999) and Zornberg et al. (2004) showed that the relation between the deviator stresses and axial strain is almost linear, (Asharei 2018). However, Asharei (2018) conducted several static drained large scale static triaxial tests, and his results displayed a strong nonlinear behaviour for the TDA. The findings of the present work, as illustrated in Figure 4, display a nonlinear behaviour as well. Furthermore, even at a 6.67% axial strain, which corresponds to 10% axial shear strain, the TDA did not reach a peak deviatoric stress value. Unlike the predicted behaviour of sandy soils where the peak point is expected to occur at a shear strain of 10% (Jia 2018).

4.2 Shear Modulus

Figure 7 shows the shear modulus reduction curves for the four tests. The shear modulus is obtained by taking the average of all shear moduli for all the cycles. In general, similar to granular soils, the shear modulus decreases nonlinearly with increasing strain amplitudes. Furthermore, as the confining pressure increases, the shear modulus curves increases for all the shear strain amplitudes. Despite the variation of the orientation of the TDA aggregates during the sample preparation for each test, the four tests have a consistent decreasing trend with each other. The shear modulus is obtained by taking the average of all shear moduli for all the cycles.

The obtained data from all the tests indicate that the TDA shear modulus of Type A TDA ranges from 613 to 2613

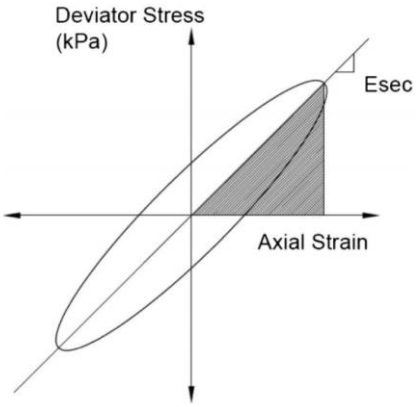

Figure 5. Schematic of typical hysteresis loop generated by the cyclic triaxial test, (Madhusudhan et al., 2017)

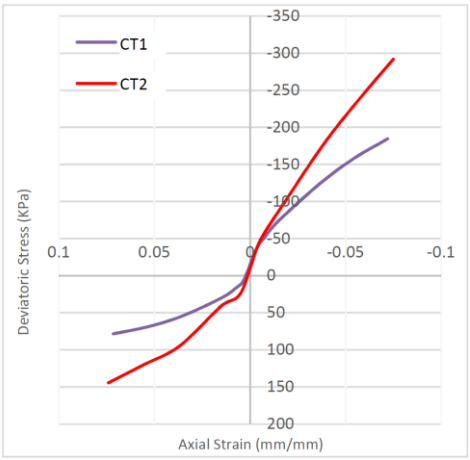

Figure 6. Backbone curves of the two tests

KPa. McCartney et al. (2017) reported that the range of shear modulus obtained by the work of Feng and Sutter (2000), Hazarika et al. (2010) and Kaneko et al. (2013) was from 160 to 2800 KPa, which is similar to the range presented in the current work.

4.3 Damping Ratio

The dampening ratio versus shear strain amplitudes is shown in Figure 8. It could be observed that the range of dampening ratios is from 10.8 to 26% at a shear strain amplitude of 0.5%. According to Seed and Idriss (1970) and Rollins et al. (1998), a typical range for dampening rations of granular soils could be from 5 to 20%, thus, this proves that TDA has a superior dampening characteristic than other natural granular soils.

The trend of CT1 test shows a continuous decrease in dampening ratios; however, CT2 test shows a decreasing then increasing trend with increasing shear amplitudes. The dampening ratio trends obtained by McCartney et al. (2017) showed a similar trend to the CT2 test.

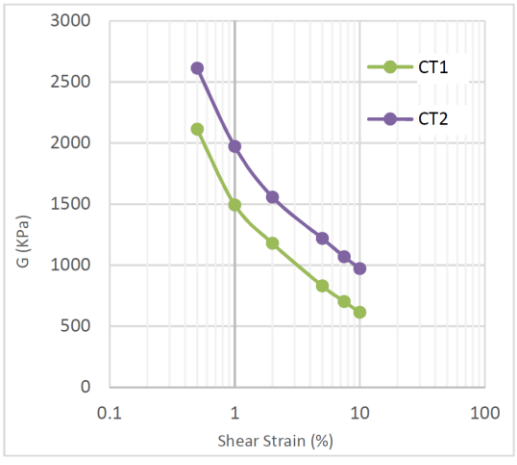

Figure 7. Variation of averaged G values with shear strain amplitudes

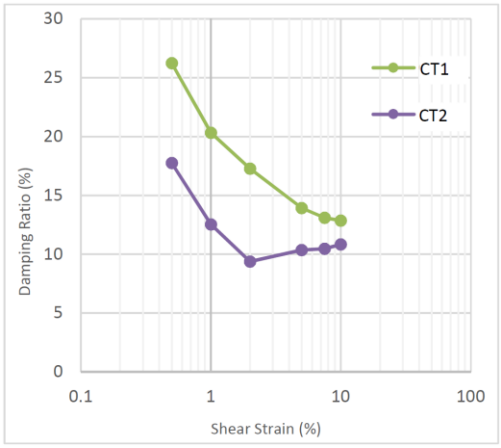

Figure 8. Damping Ratio versus shear strain amplitudes

CONCLUSIONS

Large-scale undrained consolidated cyclic triaxial tests were carried out to better understand the dynamic characteristic and behaviour of Type A TDA. The confining pressure and shear strain amplitude ranges for all the tests were 100 to 200 KPa and 0.5 to 10%, respectively. The obtained hysteretic deviatoric stress-axial strain loops showed similarity with those obtained for granular materials. The shear modulus of Type A TDA is from 613 to 2,613 KPa, which is in the range of presented shear modulus values in the literature. Furthermore, the shear modulus is decreasing with increasing shear strain amplitudes, and it has a similar trend to natural granular soils. The backbone curves for Type A TDA showed a nonlinear behaviour; nevertheless, did not show a peak point even at high shear strain magnitude. At small shear strain magnitude (0.5%), the dampening ratio range was from 10.8 to 26%, which is higher range than regular natural soils at similar shear strain magnitude. In addition, the dampening ratio of TDA could be independent of the confinement pressure.

REFERENCES

Asadi, M., Thoeni, K., & Mahboubi, A. (2018). An experimental and numerical study on the compressive behaviour of sand-rubber particle mixtures doi://doi.org/10.1016/j.compgeo.2018.08.006

Ashari Ghomi, M. (2018). Large-scale triaxial testing of sustainable TDA backfilling alternatives.

ASTM C136 / C136M-14, Standard Test Method for Sieve Analysis of Fine and Coarse Aggregates, ASTM International, West Conshohocken, PA, 2014, www.astm.org

ASTM D3999 / D3999M-11e1, Standard Test Methods for the Determination of the Modulus and Damping Properties of Soils Using the Cyclic Triaxial Apparatus, ASTM International, West Conshohocken, PA, 2011, www.astm.org

ASTM D6270-17, Standard Practice for Use of Scrap Tires in Civil Engineering Applications, ASTM International, West Conshohocken, PA, 2017, www.astm.org

Edinçliler, A., Baykal, G., & Saygılı, A. (2010). Influence of different processing techniques on the mechanical properties of used tires in embankment construction. Waste Management, 30(6), 1073-1080. doi:10.1016/j.wasman.2009.09.031

Edincliler, A., Cabalar, A. F., & Cevik, A. (2013). Modelling dynamic behaviour of sand–waste tires mixtures using neural networks and neuro-fuzzy. European Journal of Environmental and Civil Engineering, 17(8), 720-741. doi:10.1080/19648189.2013.814552

Feng, Z. -., & Sutter, K. G. (2000). Dynamic properties of granulated rubber/sand mixtures. Geotechnical Testing Journal, 23(3), 338-344. doi:10.1520/GTJ11055J

Gong, L., Nie, L., Xu, Y., Wang, H., Zhang, T., Du, C., & Wang, Y. (2019). Discrete element modelling of the mechanical behaviour of a sand-rubber mixture containing large rubber particles. Construction and Building Materials, 205, pp.574-585.

Hazarika, H., Masayuki, H., & Kazuya, Y. (2010). Investigation of tire chips-sand mixtures as preventive measure against liquefaction. In GeoShanghai International Conference 2010.

Jia, J. (2018). Soil dynamics and foundation modeling: Offshore and earthquake engineering. Springer International Publishing. doi:10.1007/978-3-319-40358-8

Kaneko, T., Orense, R., Hyodo, M., & Yoshimoto, N. (2013). Seismic response characteristics of saturated sand deposits mixed with tire chips. Journal of Geotechnical and Geoenvironmental Engineering, 139(4), 633-643.

Kowalska, M. (2016). Compactness of scrap tyre rubber aggregates in standard proctor test. Procedia Engineering, 161, 975-979.

Lee, C., Shin, H., & Lee, J. (2014). Behavior of sand–rubber particle mixtures: Experimental observations and numerical simulations. International Journal for Numerical and Analytical Methods in Geomechanics, 38(16), 1651-1663. doi:10.1002/nag.2264

Lee, J. H., Salgado, R., Bernal, A., & Lovell, C. W. (1999). Shredded tires and rubber-sand as lightweight backfill. Journal of Geotechnical and Geoenvironmental Engineering, 125(2), 132-141. doi:https://doi.org/10.1061/(ASCE)1090-0241(1999)125:2(132)

Madhusudhan, B. R., Boominathan, A., & Banerjee, S. (2019). Properties of Sand–Rubber tyre shreds mixtures for seismic isolation applications. Paper presented at the Soil Dynamics and Earthquake Geotechnical Engineering, 267-274.

Madhusudhan, B. R., Boominathan, A., & Subhadeep, B. (2017). Static and large-strain dynamic properties of Sand–Rubber tire shred mixtures. Journal of Materials in Civil Engineering, 29(10), 04017165. doi:10.1061/(ASCE)MT.1943-5533.0002016

Masad, E., Taha, R., Ho, C., & Papagiannakis, T. (1996). Engineering properties of tire/soil mixtures as a lightweight fill material. Geotechnical Testing Journal, 19(3), 297-304.

Mashiri, M. S., Vinod, J. S., & Neaz Sheikh, M. (2016). Liquefaction potential and dynamic properties of sand-tyre chip (STCh) mixtures. Geotechnical Testing Journal, 39(1), 69-79. doi:10.1520/GTJ20150031

MATLAB and Statistics Toolbox R2018b (2018), The Math Works, Inc., Natick, Massachusetts, United States

McCartney, J. S., Ismaail, G., Fox, P. J., Sanders, M. J., Thielmann, S. S., & Sander, A. C. (2017). Shearing behavior of tire-derived aggregate with large particle size. II: Cyclic simple shear. Journal of Geotechnical and Geoenvironmental Engineering, 143(10), 04017079.

Meles, D., Chan, D., Yi, Y., & Bayat, A. (2015). Finite-element analysis of highway embankment made from tire-derived aggregate. Journal of Materials in Civil Engineering, 28(2), 04015100.

Takano, D., Chevalier, B., & Otani, J. (2015). Experimental and numerical simulation of shear behavior on sand and tire chips

Wu, W. Y., Benda, C. C., & Cauley, R. F. (1997). Triaxial determination of shear strength of tire chips. Journal of Geotechnical and Geoenvironmental Engineering, 123(5), 479-482. doi:5(479)

Youwai, S., & Bergado, D. T. (2003). Strength and deformation characteristics of shredded rubber tire – sand mixtures. Canadian Geotechnical Journal, 40(2), 254-264. doi:10.1139/t02-104

Zornberg, J., Cabral, A., & Viratjandr, C. (2004). Behaviour of tire shred - sand mixtures. Canadian Geotechnical Journal, 41(2), 227-241.